phys. stat. sol. (a) **201**, No. 1, 72–79 (2004) / **DOI** 10.1002/pssa.200306692

Characterization of $ZnAl_2O_4$: Tb luminescent films deposited by ultrasonic spray pyrolysis technique

M. García-Hipólito[1], **A. Corona-Ocampo**[1], **O. Alvarez-Fregoso**[*, 1], **E. Martínez**[1], **J. Guzmán-Mendoza**[1], and **C. Falcony**[2]

[1] Instituto de Investigaciones en Materiales., UNAM, A.P. 70-360 Coyoacán 04510 México
[2] Departamento de Física, CINVESTAV-IPN, Apdo. Postal 14-740, 07000. México D.F.

Received 5 July 2003, revised 27 August 2003, accepted 3 September 2003
Published online 30 December 2003

PACS 78.55.Hx, 81.05.Hd, 81.15.Rs, 81.20.Rg

The preparation and characterization of terbium doped zinc aluminate photoluminescent films obtained by ultrasonic spray pyrolysis deposition process are described. Variations on doping concentrations in the start spraying solution and substrate temperatures were studied. XRD measurements on these films showed that the crystalline structure depends on the substrate temperature. For an excitation wavelength of 242 nm, all the photoluminescence spectra show peaks located at 488 nm, 546 nm, 589 nm and 621 nm. The photoluminescence intensity reaches values practically constant for the samples deposited at substrate temperatures higher than 400 °C. In this case, concentration quenching of the photoluminescence appears at doping concentrations greater than 0.93 atomic percent into the films. The surface morphology characteristics of the films deposited on glass and silicon substrates, as a function of the deposition temperature, are presented.

1 Introduction

Luminescence from rare earth-doped phosphors has generated much interest in recent years, because of their many technological applications. These materials are promising candidates for optoelectronic devices such as electroluminescent flat panel displays, color plasma display panels, etc [1]. Rare earth doped oxides are some of the most promising luminescent materials for these applications. In contrast to sulfur-based luminescent materials, oxides are chemically inert to plasmas commonly used in plasma operated panels and do not contaminate the electron emitters in field emission displays [2]. Rare earth ions provides fixed emission lines, which are almost insensitive to the influence of surroundings due to the shielding effect of the outer 5s and 5p orbitals [3].

Luminescent coatings as compared to powder phosphors offer advantages such as no outgassing problems, good adhesion to the substrate, better thermal stability and present uniform characteristics across the covered area [2].

The ultrasonic spray pyrolysis technique is a well-established process for depositing films [4]. Some advantages of this process are: a high deposition rate; the possibility to coat large areas; its low cost; its ease of operation; the quality of the coatings obtained.

This technique has been used to deposit luminescent films of materials such as $Y_3Al_5O_{12}$: Tb, Eu or Ce [5] ZnO: Tb [6], ZrO_2: Tb [7], Al_2O_3: $CeCl_3$ [8], Al_2O_3: Eu [9], ZrO_2: Eu [10], ZnS: Mn [11], ZrO_2: Mn, Cl [12], etc.

[*] Corresponding author: e-mail: oaf@servidor.unam.mx

$ZnAl_2O_4$ (zinc aluminate) is a well-known wide-bandgap semiconductor with a spinel structure. This material has a close-packed face centered cubic structure with Fd3m space group symmetry [13]. The optical bandgap of polycrystalline $ZnAl_2O_4$ is 3.8 eV [14]. This indicates that zinc aluminate is transparent for light possessing wavelengths > 320 nm which makes it useful in ultraviolet photoelectronic devices [15]. Zinc aluminate is widely used as ceramic, electronic and catalytic materials. This material is employed in various catalytic reactions such as cracking, dehydration, hydrogenation, and dehydrogenation in chemical and petrochemical industries [16, 17].

There has been noticeable investigation involving both experimental and theoretical studies on spinel oxides like magnesium aluminate, but there are scarce works on zinc aluminate. The studied characteristics of these materials are the electronic structure, the optical spectra and the crystal structure [13, 18, 19]. Regarding the luminescent properties of zinc aluminate there are very few reported studies [20, 21, 22]. These studies have been carried out on samples in the form of powder. There are hardly any studies reporting on the general properties of zinc aluminate films [23]. To our knowledge, reported contributions about zinc aluminate luminescent films are unknown.

In this work, the synthesis and characterization of the photoluminescent Tb doped zinc aluminate coatings deposited by the ultrasonic spray pyrolysis technique are presented. The influence that some deposition parameters (substrate temperature and doping concentration) play on the luminescent characteristics is also studied.

2 Experimental details

Films of terbium doped zinc aluminate were deposited by a ultrasonic spray pyrolysis technique described earlier [24]. Basically, this technique consists of an ultrasonic generator used to produce a mist from the spraying solution. This mist is carried to a hot substrate placed on a tin bath through a tubing setup using humid air as a carrier gas (10 liters/minute). When the mist of the solution gets in touch with the hot substrate, the solvents in the solution are vaporized producing a solid coating on the substrate. The nozzle in this system is localized approximately 1 cm above the substrate. The spraying solution consisted of 0.05 M zinc acetate and aluminum chloride in de-ionized water as solvent. Doping with Tb was achieved by adding $TbCl_3 \cdot 6H_2O$ to the spraying solution in the range of 0 to 50 atomic percent (a/o) in relation to the Zn content in this solution. The solution flow rate was 3 ml/minute for all cases. The substrate temperature (T_s) during deposition was in the range from 350 ºC to 550 °C; the substrates used were Corning 7059 glass slides and Si (100) wafer pieces. The deposition time was adjusted (4 to 6 minutes) to deposit films with approximately the same thickness. The thickness of the films studied was about 5 μm as measured by a Sloan Dektak IIA profilometer. The chemical composition of the films was measured with a Cambridge-Leica electron microscope mod. Stereoscan 440, equipped with a Beryllium window X-ray detector, using Energy Dispersive Spectroscopy (EDS). The standard used for the EDS measurements was the Multi-element X-ray Reference Standard (Microspec), Serial 0034, part No. 8160-53. The surface morphology was analyzed by means of the scanning electron microscopy (SEM) cited above. The crystalline structure features of the deposited films were analyzed by X-ray diffraction (XRD), using a Siemens D-5000 diffractometer with wavelength radiation of 1.5406 Å (Cu k_α). The excitation and emission photoluminescence (PL) spectra were obtained using a Perkin-Elmer LS50B fluorescence spectrophotometer. Light of 242 nanometers (nm) was found to be suitable as excitation source for these measurements. All PL spectra were obtained at room temperature. All PL spectra were corrected for the detection system response.

3 Results and discussion

The surface morphology of $ZnAl_2O_4$: Tb (0.93 a/o) coatings deposited on glass substrates are presented in Fig. 1. SEM micrographs show the samples deposited at: 350 °C (a); 450 °C (b); and 550 °C (c). It is possible to observe rough but continuous coatings with good adherence to the substrate. This figure shows that the surface morphology of the layers depends on substrate temperature. Coatings deposited at

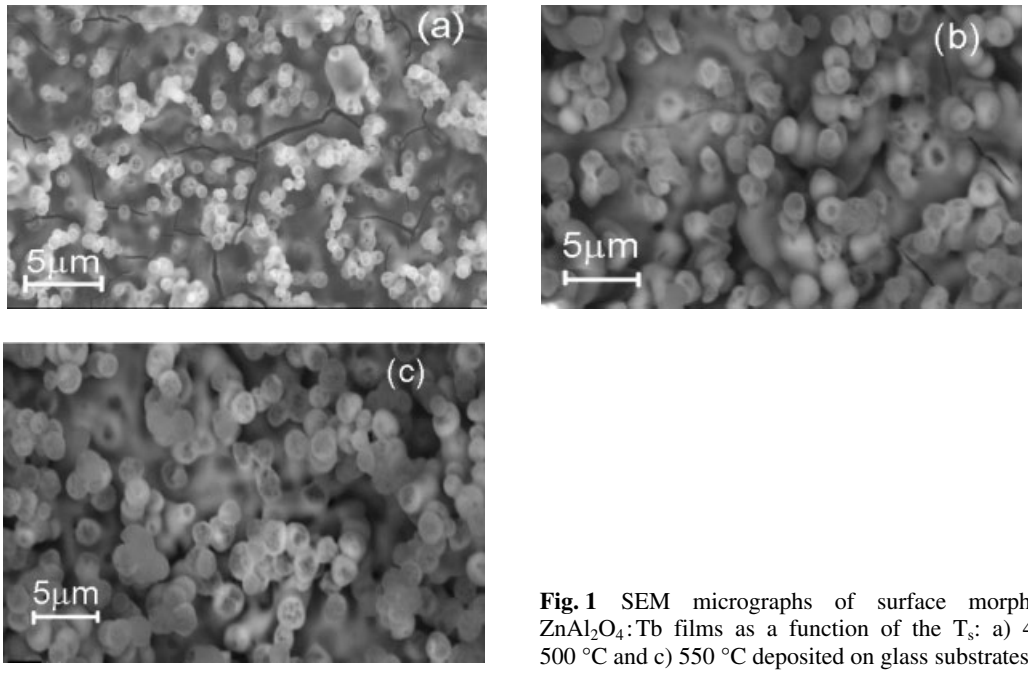

Fig. 1 SEM micrographs of surface morphology of $ZnAl_2O_4$:Tb films as a function of the T_s: a) 400 °C, b) 500 °C and c) 550 °C deposited on glass substrates.

350 °C and 450 °C present some cracks. By increasing the substrate temperature to 550 °C, cracks disappear and a relatively more dense material is reached. These features could be explained because at higher substrate temperature the deposited radicals are characterized by higher surface kinetic energy, which permits them better accommodation and consequently produces a better processed, denser material.

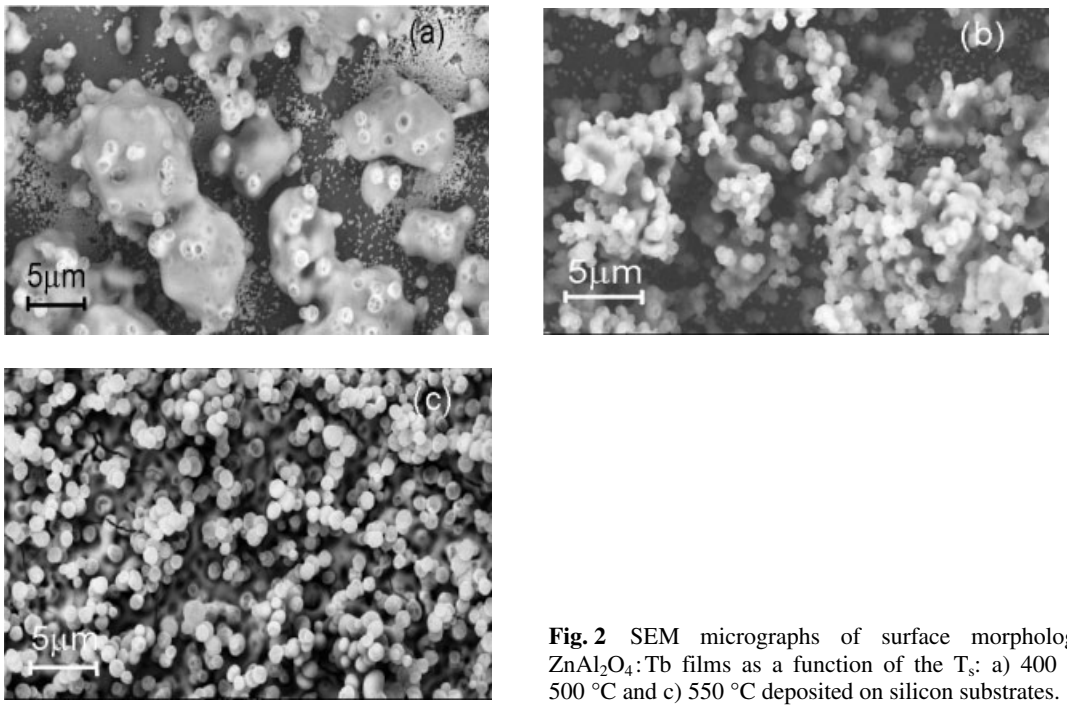

Fig. 2 SEM micrographs of surface morphology of $ZnAl_2O_4$:Tb films as a function of the T_s: a) 400 °C, b) 500 °C and c) 550 °C deposited on silicon substrates.

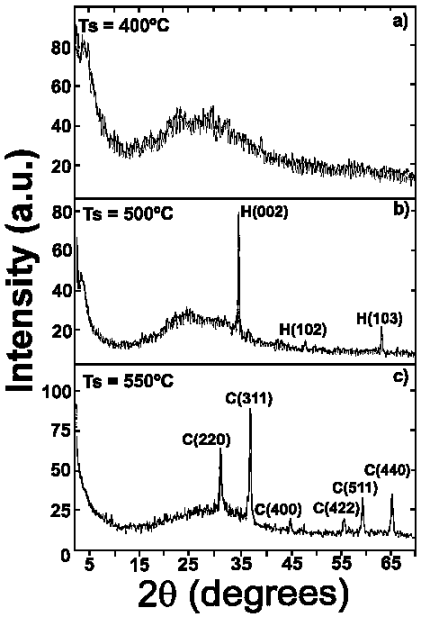

Fig. 3 XRD patterns for $ZnAl_2O_4$: Tb (0.93 a/o) films at three different substrate temperature, T_s: 400 °C, 500 °C and 550 °C. (H = hexagonal, C = cubic).

The Fig. 2a–c shows SEM images from surface morphology of the $ZnAl_2O_4$: Tb (0.93 a/o) coatings synthesized on silicon substrates at these temperatures: 350 °C (a); 450 °C (b); and 550 °C (c). Samples deposited at lower substrate temperature (350 °C) show an incomplete covering of the substrate. As the deposition temperature is increased (450 °C and 550 °C) a complete covering of the substrate is reached. It is possible to distinguish some differences with the surface features of those coatings deposited on glass substrates. In this case, the sample deposited at 550 °C presents a rough and continuous surface, but more finely granulated. The surface particles have a more spherical form than those of the layers deposited on glass substrates.

XRD measurements carried out on the Tb doped $ZnAl_2O_4$ coatings deposited by spray pyrolysis technique are presented in Fig. 3a–c. These XRD patterns are shown for $ZnAl_2O_4$: Tb films (0.93 a/o inside the films) at these three different substrate temperatures: 400 °C; 500 °C; and 550 °C. The Tb doped zinc aluminate coatings remain in the amorphous state when deposited at substrate temperatures up to 400 °C (Fig. 3a); as the substrate temperature is increased to 500 °C, some peaks corresponding to hexagonal phase of ZnO (zincite, ICCD Card File No. 36–1451) are observed in Fig. 3b. In the case of the sample deposited at 550 °C (Fig. 3c) only a cubic spinel crystalline phase of $ZnAl_2O_4$ (gahnite) was found (ICCD Card File No. 05-0669 [25]). The calculated lattice parameters (a = b = c = 8.0859 Å) for the cubic spinel phase in the films deposited at 550 °C are in agreement with the reported values (a = b = c = 8.0848 Å) [25]. Furthermore, it promoted the crystal growth of this material with a preferential (311) orientation normal to the coatings surface.

EDS measurements were performed on films deposited on (1 0 0) n-type silicon single crystals substrates in order to evaluate the oxygen content in the coatings. The obtained results are shown in Tables 1 and 2. Table 1 summarizes the relative chemical content of: oxygen; zinc; aluminum; terbium; and chlorine, present in the films as a function of the content of the $TbCl_3$ inserted in the spraying solution.

Table 1 Atomic percent content of the oxygen, zinc, aluminum, terbium and chlorine in the terbium-doped zinc aluminate films as measured by EDS for different $TbCl_3$ concentrations in the spraying solution. In this case the substrate temperature was 550 °C.

$TbCl_3$ concentration in the spraying solution (a/o)	Oxygen	Zinc	Aluminum	Terbium	Chlorine
0	56.89	13.17	27.23	00.00	02.71
5	59.19	11.32	26.01	00.50	02.98
10	57.71	11.86	25.90	00.86	03.67
15	59.06	10.52	25.67	00.93	03.82
20	60.27	09.95	24.23	01.10	04.45
40	57.32	09.71	23.52	02.48	06.97
50	60.06	07.83	20.58	02.80	09.03

Table 2 Atomic percent content of the oxygen, zinc, aluminum, terbium and chlorine in the terbium-doped zinc aluminate films as determined by EDS for different substrate temperatures. In this case, the $TbCl_3$ concentration in the spraying solution was 15 a/o.

substrate temperature (°C)	Oxygen	Zinc	Aluminum	Terbium	Chlorine
350	54.88	10.60	17.71	02.39	14.42
400	56.45	09.87	18.62	01.91	13.15
450	57.12	10.79	19.16	01.46	08.05
500	58.35	12.02	22.93	01.01	06.92
550	59.06	10.52	25.67	00.93	03.82

A reduction of the relative content of zinc and aluminum, and an increase in the relative contents of oxygen, terbium and chlorine is observed when the doping concentration rises. The substrate temperature, in this case, was 550 °C. Table 2 presents results similar to those in Table 1, but as a function of the substrate temperature, keeping the doping concentration ($TbCl_3$, 15 a/o) constant in the starting solution. In this case, we observe an increase in the relative content of oxygen and aluminum, and a reduction in the relative content of terbium and chlorine, as the substrate temperature increases. The relative content of zinc is maintained constant.

The excitation spectra for the photoluminescence of $ZnAl_2O_4$: Tb coatings synthesized at 550 °C with 0.93 a/o of Tb inside the films, are shown in the Fig. 4 (all samples used in the luminescence characterization were deposited on silicon substrates). The emission wavelength was fixed at: 546 nm (a); 488 nm (b); 589 nm (c); and 621 nm (d), respectively. It is possible to distinguish asymmetrical broad bands with wavelength ranging from 225 nm to 400 nm. In these broad bands are noted some peaks and shoulders centered at: 242 nm; 257 nm; 268 nm; 278 nm; and 350 nm. We can observe the $4f^8 \rightarrow 4f^75d$ transition, which corresponds to the peaks or shoulders between 225 nm and 300 nm [26]. In this case, the dominant peak (Fig. 4a) appears at around 242 nm, which is due to this transition of Tb^{3+} affected by the surroundings of Tb^{3+} ions in $ZnAl_2O_4$ matrix. Since the outer shell electrons screen the electrons of 4f shells, the presence of the surrounding lattice has little effect on the 4f-4f absorptions. In addition, the parity-selection rule forbids these transitions. However, some 4f-4f absorptions features are observed at around 350 nm. This characteristic is more notable in the spectrum of Fig. 4b. This effect is probably attributed, once again, to the influence of the surroundings of Tb^{3+} ions in the zinc aluminate matrix. We choose 242 nm wavelength radiations to excite the coatings studied in this contribution.

In the Fig. 5a, representative PL emission spectrum for Tb doped zinc aluminate films is shown. This spectrum exhibits four main bands centered at: 488 nm ($^5D_4 \rightarrow {}^7F_6$); 546 nm ($^5D_4 \rightarrow {}^7F_5$); 589 nm ($^5D_4 \rightarrow {}^7F_4$); and 621 nm ($^5D_4 \rightarrow {}^7F_3$), which correspond to electron transitions of the Tb^{3+} ions. The emission at 546 nm is the strongest. In these cases, the films were prepared at substrate temperature of 550 °C, the concentration doping was 0.93 a/o inside the films and $\lambda_{exc} = 242$ nm. The broad band centered at approximately 450 nm is associated to host lattice [27]. In this case, the line emissions from $^5D_3 \rightarrow {}^7F_j$ transitions of the Tb^{3+} ions are absent and only that from $^5D_4 \rightarrow {}^7F_j$ ($j = 3, \ldots, 6$) transitions are observed. The luminescence emission from the films studied is very strong and easily appreciated by the

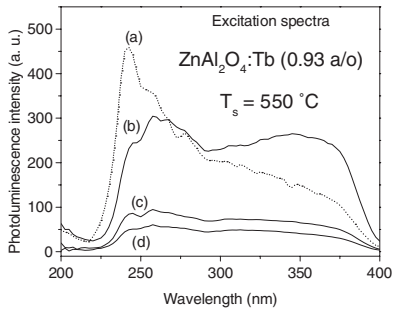

Fig. 4 Excitation spectra of $ZnAl_2O_4$: Tb (0.93 a/o) films deposited at $T_s = 550$ °C, λ_{em} = (a) 546 nm, (b) 488 nm, (c) 589 nm and (d) 621 nm.

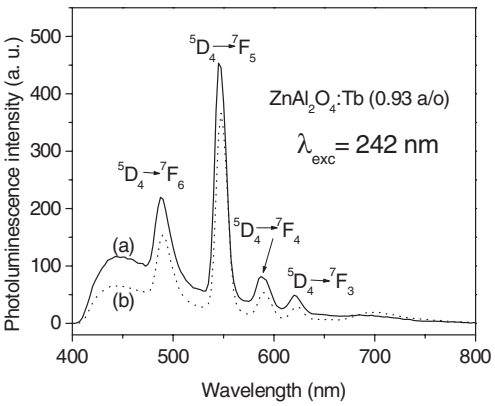

Fig. 5 a) Typical PL spectrum for $ZnAl_2O_4$:Tb (0.93 a/o) films synthesized at $T_s = 550$ °C, $\lambda_{exc} = 242$ nm. b) PL spectrum for $ZnAl_2O_4$: Tb (15 a/o) powders.

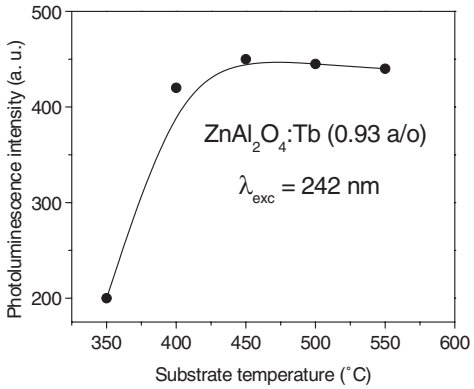

Fig. 6 Substrate temperature dependence of PL emission intensity of $ZnAl_2O_4$: Tb (0.93 a/o) films, $\lambda_{exc} = 242$ nm.

naked eye in normal room lightening when excited with a 4 watts UV-mercury lamp (254 nm). In the Fig. 5b, shown for comparison purposes, the emission spectrum is obtained from similar material in the form of powders (these powder samples were synthesized in identical conditions to that of the reference [21]) and is measured in the same conditions as the spectrum in the Fig. 5a. The emission intensity from the $ZnAl_2O_4$: Tb films is higher, in all of cases, than that coming from the powders. This result indicates that the PL sensitivity of the films is better than that of the powders.

The behavior of PL emission intensity (green peak centered at 546 nm) of $ZnAl_2O_4$: Tb coatings, as a function of the substrate temperature, is shown in the Fig. 6. The PL emissions rise when increasing the deposition temperature up to 450 °C, then a saturation effect of the emission intensity is observed. In this case, the value of doping concentration in the deposited film was 0.93 a/o and $\lambda_{exc} = 242$ nm. As the substrate temperature rises, an improved crystallization of the host material is obtained, as shown by X-ray diffractograms. Also, a reduction of chlorine incorporated inside the samples is observed as indicated by the EDS measurements. Both effects could contribute to the optimal incorporation and distribution of the terbium ions as an atomic impurity inside the host lattice. This could be a factor to maintain, more or less constant, the PL emission intensity as a function of the deposition temperature (starting from 450 °C). Moreover, it is possible note that luminescent emissions are observed despite the crystalline structure of films studied. Terbium doped zinc aluminate films deposited at 350 °C (non-crystalline or amorphous) show typical emission from the trivalent terbium ion. Similar behavior is observed for films deposited at higher substrate temperatures (500 and 550 °C), with crystalline structures corresponding to zinc oxide (hexagonal phase) and zinc aluminate (cubic phase). In the last case, the PL emission is more intense. At this point it is convenient to consider that the luminescence spectrum of the trivalent terbium ion is only slightly influenced by surrounding ligands of the host lattice. This is due to the fact that electronic transitions of Tb involve only a redistribution of electrons within the inner 4f sub-shell [28]. An attempt to deposit films at substrate temperature higher than 550 °C (600 °C) was made. The obtained material was powdery, porous and non-adherent to the substrate. In all probability, at this relatively high temperature, the complete chemical reaction is carried out in the vapor phase in a close region to the substrate. This produces only a fine powder of the material completely processed, which falls on the substrate and does not constitute a solid film.

Figure 7 show the variation of PL emission intensity (band centered at 546 nm) for Tb doped zinc aluminate films, as a function of doping concentration. $T_s = 550$ °C and $\lambda_{exc} = 242$ nm. In this figure, a maximum value of the PL emission intensity for 15 a/o of $TbCl_3$ in the spraying solution (0.93 a/o inside the films as measured by EDS) is observed. It is also possible to note a concentration quenching for higher values than 15 a/o of $TbCl_3$ in the initial solution. In this respect, Dexter and Schulman [29] have

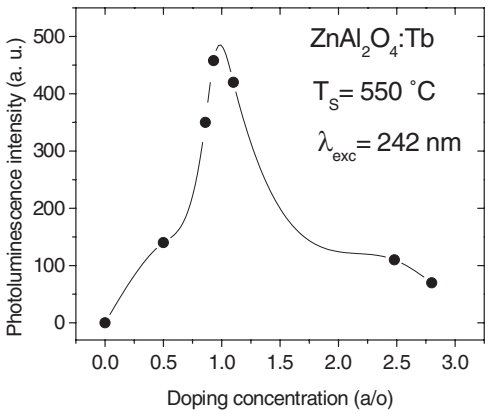

Fig. 7 Doping concentration dependence of PL emission intensity of $ZnAl_2O_4$: Tb films, $T_s = 550$ °C, $\lambda_{exc} = 242$ nm.

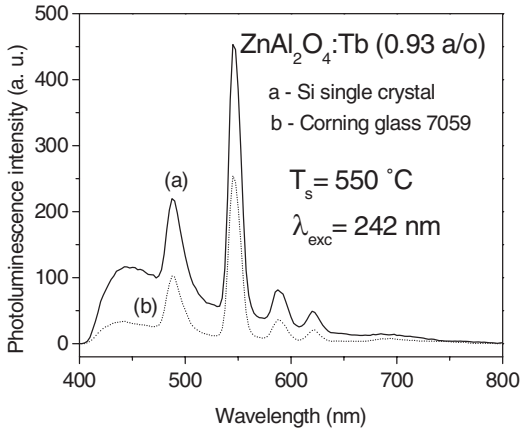

Fig. 8 Comparison between the PL emission intensity of $ZnAl_2O_4$: Tb (0.93 a/o) films deposited on (a) silicon substrates and (b) glass substrates, $T_s = 550$ °C, $\lambda_{exc} = 242$ nm.

suggested that: at high impurities concentration, the energy can migrate from one luminescent center to another and reach a sink, from which nonradiative processes can dissipate this energy. In this case, as the terbium content is increased in the host lattice, a resonant energy transfer effect between these ions is favored. Then, the aggregation of activators at high concentrations, may change some activators to quenchers and induce the quenching effect. This concentration quenching will not appear at low concentrations because the average distance between activators is so large that the migration is prevented, thus, the killers are not reached [30].

Figure 8 presents the behavior of the PL emission spectra for Tb doped zinc aluminate films, as a function of the kind of substrate used; $T_s = 550$ °C, the doping concentration was 0.93 a/o and $\lambda_{exc} = 242$ nm. It is interesting that, changing the substrate from glass to silicon caused a noted increase in the PL emission intensity of films deposited under the same conditions. It was also noted that, the peak positions and peak-width did not change as the substrate changed. A factor in the explanation of this effect could be the existence of the non-negligible contribution of the reflected emission of the PL signal at the $ZnAl_2O_4$: Tb/silicon interface. This is absent in the transparent $ZnAl_2O_4$: Tb/silicon interface. In addition, it is probable that this difference in emissions intensity could be related to the differences in surface morphology of the samples deposited on the glass and silicon substrates shown in Figs. 1c and 2c. More work is in progress to sufficiently elicit this point.

4 Conclusions

Zinc aluminate films doped with Tb were used for observing green PL emissions and deposited from ultrasonic spray pyrolysis. These observations were obtained at a high deposition rate of up to 1 μm per minute. SEM micrographs showed rough, but dense and continuous films. Their surface features depended on the substrate temperature and the type of substrate employed. XRD measurements of these films show that their crystalline structure depended on the deposition temperature. At low temperatures they were not in the crystalline state and when the deposition temperature was increased (up to 550 °C) they transformed to cubic phase of the $ZnAl_2O_4$ (gahnite). The luminescence emission of Tb doped zinc aluminate films is characteristic for the Tb^{3+} ion transitions between the levels $^5D_4 \rightarrow {}^7F_j$ (j = 3, …, 6). An increase of the PL emission intensity as the substrate temperature rises was observed (up to 450 °C). Beginning at this temperature, the PL intensity emission is almost constantly maintained. It was observed that concentration quenching happens if the activator concentration increases above the optimum doping

concentration, 0.93 a/o, as measured by EDS. In addition, the PL emission intensity of the samples grown on silicon substrates was higher than that from samples deposited on glass substrates. It was also confirmed that zinc aluminate is an adequate host matrix for rare earth ions, as active centers, to cause luminescence emissions. To our knowledge, there are no written reports on the synthesis and characterization of terbium doped-zinc aluminate luminescent films.

Acknowledgements The authors would like to thank to Leticia Baños for X-ray diffraction measurements, Sarita Jimenez, Marcela Guerrero and Juan García-Coronel for their technical support.

References

[1] C. N. King, Conference Record of the International Display Research Conference, San Diego 155 (1985).
[2] G. A. Hirata, J. McKittrick, M. Avalos-Borja, J. M. Siqueiros, and D. Devlin, Appl. Surf. Sci. **113/114**, 509 (1997).
[3] G. H. Dieke, Spectra, and Energy Levels of Rare Earth Ions in Crystals, Interscience (New York, 1968).
[4] J. C. Viguie and J. Spitz, J. Electrochem. Soc. **122**, 585 (1975).
[5] A. Esparza, M. García, and C. Falcony, Thin Solid Films **325**, 14 (1998).
[6] A. Ortiz, C. Falcony, M. García, and A. Sánchez, J. Phys. D: Appl. Phys. **20**, 670 (1987).
[7] M. García-Hipólito, R. Martínez, O. Álvarez-Fregoso, E. Martínez, and C. Falcony, J. Lumin. **93**, 9 (2001).
[8] C. Falcony, M. García, A. Ortiz, O. Miranda, I. Gradilla, G. Soto, L. Cota-Araiza, M. H. Farías, and J. C. Alonso, J. Electrochem. Soc. **141**, 2860 (1994).
[9] E. Martínez, M. García, F. Ramos-Brito, O. Alvarez-Fregoso, S. López, S. Granados, J. Chavez-Ramírez, R. Martínez M., and C. Falcony, phys. stat. sol. (b) **220**, 667 (2000).
[10] M. García-Hipólito, E. Martínez, O. Álvarez-Fregoso, C. Falcony, and M. A. Aguilar-Frutis, J. Mater. Sci. Lett. **20**, 1799 (2001).
[11] C. Falcony, M. García, A. Ortiz, and J. C. Alonso, J. Appl. Phys. **72** (4), 1525 (1992).
[12] M. García-Hipólito, O. Alvarez-Fregoso, E. Martínez, C. Falcony, and M. A. Aguilar-Frutis, Opt. Mater. **20**, 113 (2002).
[13] R. J. Hill, J. R. Craig, and G. V. Gibbs, Phys. Chem. Miner. **4**, 317 (1979).
[14] S. K. Sampath and J. F. Cordaro, J. Am. Ceram. Soc. **81**, 649 (1998).
[15] S. Mathur, M. Veth, M. Hass, H. Shen, N. Lecerf, V. Huch, S. Hufner, R. Haberkorn, H. P. Beck, and M. Jilabi, J. Am. Ceram. Soc. **84**, 1921 (2001).
[16] T. El-Nabarawy, A. A. Attia, and M. N. Alaya, Mater. Lett. **24**, 319 (1995).
[17] B. S. Girgis, A. M. Youssef, and M. N. Alaya, Surf. Technol. **10**, 105 (1980).
[18] S. K. Sampath, D. G. Kanhere, and R. Pandey, J. Phys.: Condens. Matter. **11**, 3635 (1999).
[19] S. Itoh, H. Toki, Y. Sato, K. Morimoto, and T. Kishino, J. Electrochem. Soc. **138**, 1509 (1991).
[20] H. Matsui, C. N. Xu, and H. Tateyama, Appl. Phys. Lett. **78**, 1068 (2001).
[21] M. Zawadski, J. Wrzyszcz, W. Strek, and D. Hreaniak, J. Alloys Compd. **323/324**, 279 (2001).
[22] W. Strek, P. Deren, A. Bednarkiewicz, M. Zawadski, and J. Wrzyszcz, J. Alloys Compd. **300/301**, 456 (2000).
[23] A. R. Phani, M. Passacantando, and S. Santucci, Mater. Chem. Phys. **68**, 66 (2001).
[24] M. Langlet and J. C. Joubert, in: Chemistry of Advanced Materials, edited by C. N. R. Rao, Blackwell Science (Oxford, England, 1993) pp. 55.
[25] Powder Diffraction File Card No. 05-0669, International Center for Diffraction Data, Newtown Square, PA, 1990.
[26] R. Reisfeld, J. Res. Natl. Bur. Stand. A, Phys. Chem. A **76**, 613 (1972).
[27] M. García-Hipólito, C. D. Hernández-Pérez, O. Álvarez-Fregoso, E. Martínez, J. Guzmán-Mendoza, and C. Falcony, Opt. Mater. **22**, 345 (2003).
[28] S. A. Studenikin and M. Cocivera, Thin Solid Films, **394**, 264 (2001).
[29] D. L. Dexter and J. H. Schulman, J. Chem. Phys. **22**, 1063 (1954).
[30] G. Blasse and B. C. Grabmaier, Luminescent Materials (Springer-Verlag, Berlin, 1994).